JOURNAL OF GEOPHYSICAL RESEARCH, VOL. 106, NO. A10, PAGES 20,947–20,955, OCTOBER 1, 2001

The correlation between solar energetic particle peak intensities and speeds of coronal mass ejections: Effects of ambient particle intensities and energy spectra

S. W. Kahler
Space Vehicles Directorate, Air Force Research Laboratory, Hanscom Air Force Base, Massachusetts

Abstract. The correlation of peak intensities of solar energetic particle (SEP) events with the speeds of the associated coronal mass ejections (CMEs) is understood to be a result of SEP acceleration at shocks driven by the CMEs. However, the peak SEP intensities associated with CMEs of a given speed vary over $\sim$ 4 orders of magnitude. We examine a database of 71 $E > 10$ MeV SEP events observed with the GOES satellite to determine whether enhanced ambient SEP intensities at the times of the CMEs and/or variations among SEP event spectra contribute to the large range of peak SEP event intensities. A statistical analysis shows that enhanced ambient SEP intensities may be a contributing factor to the range of SEP events of higher peak intensities, probably by providing sources of energetic seed particles for the shock acceleration process. Another factor is the variation of energy spectra among the SEP events, which generally have harder spectra with increasing peak intensities. The observed increase of peak SEP intensities and hardening of peak SEP spectra with increasingly westward solar source regions is only a minor factor in the range of SEP peak intensities in the CME speed correlation.

1. Introduction

The correlation of peak solar energetic ($E > 10$ MeV) particle (SEP) intensities with speeds of associated coronal mass ejections (CMEs) has been established in several studies of gradual SEP events [*Reames,* 1999; *Kahler,* 1996]. Figure 1 [*Reames,* 2000] shows a log-log plot of the 2 and 20 MeV proton peak intensities against the associated CME speeds for two separate studies of gradual SEP events. Since the SEPs are assumed to be accelerated in shocks driven by the CMEs [*Reames,* 1999, 2000], the correlation is not surprising, although there are several obvious sources of error in such a plot. First, the CME speeds are measured in projection on the plane of the sky and show a statistical increase with increasing central meridian distances of the CME source regions [*Gopalswamy et al.,* 2000]. Second, it is both the Alfven speed in the solar wind and the CME speed relative to the ambient solar wind speed that determine whether the CME drives a shock. In addition, the CME speeds are proxies for the shock speeds, so that when the shock speeds are directly measured or inferred, their correlation with SEP intensities is better than that of the CME speeds with SEP intensities [*Reames et al.,* 1997]. While these factors must contribute to the observed scatter of points in Figure 1, we see that for a given CME speed the range in associated peak SEP intensities extends over 3 or 4 orders of magnitude, suggesting that factors other than CME speed are important for the peak SEP intensities.

Kahler et al. [1999] used 32 IMP 8 proton events with $28 < E < 43$ MeV and associated west limb CMEs observed with the SMM coronagraph to address the large scatter in the SEP/CME plots. They searched for other contributing factors in a subset of 17 SEP events correlated with CMEs in the restricted CME speed range of 650–850 km s^{-1}. The only significant factor appeared to be that of an enhanced ambient SEP intensity at the time of the CME which produced the subsequent SEP event. Of the four cases in which the ambient 20-80 MeV intensities were enhanced, three occurred during the three largest of the 17 SEP events. *Kahler et al.* [2000] extended this result by correlating the peak intensities of all 32 SEP events with the ambient $0.5 < E < 4$ and $20 < E < 80$ MeV IMP 8 Goddard Medium Energy (GME) detector counting rates. Comparing logs of SEP event peak intensities and of ambient counting rates, they found correlations of $r = 0.40$ and $r = 0.59$, respectively, for the two energy ranges. This suggests that the ambient SEP population at the time of a fast CME is an important factor in determining the intensity of the SEP event produced by the CME-driven shock.

Paper number 2000JA002231.

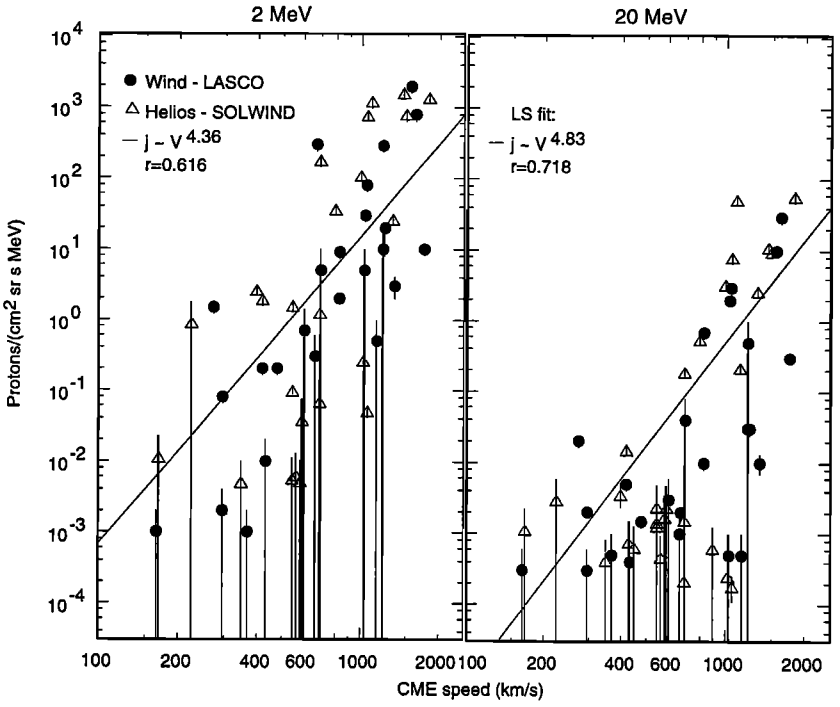

Figure 1. Plot of peak 2 and 20 MeV proton intensities versus associated coronal mass ejection (CME) speeds for two different data sets. LASCO, •; SOLWIND, △; From *Reames* [2000].

Shock acceleration theory shows that both the upstream and downstream SEP intensities at a given momentum p are proportional to $(p/p_0)^{-\gamma}$, where γ is a function of the shock compression ratio and p_0 is the injection momentum [*Lee*, 1997]. Thus, enhanced shock SEP intensities result when the shock acts on a population of energetic SEPs as the seed particles. There have been a number of suggestions or observations supporting the basic idea that heliospheric shock acceleration works more efficiently when the shock acts on a population of energetic or preaccelerated particles. Interstellar pickup ions [*Giacalone and Jokipii*, 1997] and transient SEP events [*Desai et al.*, 1998; *Lario et al.*, 2000] have been suggested as candidate energetic seed populations for acceleration to MeV energies at corotating interaction region (CIR) shocks. *Mason et al.* [1999] offered suprathermal ions from impulsive SEP events as a source population for gradual SEP events in which high ^{3}He/^{4}He ratios are observed at 1 AU. However, the possibility that transient gradual SEP populations could also act as seed particles for further acceleration by CME-driven shocks was only recently tested with the limited data set of 32 SEP events associated with SMM CMEs [*Kahler et al.*, 2000].

SEP spectral variations from event to event should also be expected to contribute to the scatter of data points in Figure 1. It is well known that SEP peak energy spectral indices range from $\sim$ 2 to 6 for assumed power laws in energy and that the spectral indices vary with solar source longitude [*Van Hollebeke et al.*, 1975; *Cane et al.*, 1988]. In addition, intense SEP events show a maximum-intensity plateau at low energies resulting from scattering by self-generated waves [*Reames and Ng*, 1998] in the shock. At high energies a spectral knee characterizes the energy at which wave growth is insufficient to prevent the escape of SEPs from the shock region. The energy of the spectral knee can vary among different events from 20 MeV to 1 GeV [*Reames*, 2000]. Thus variations in energy spectra should make an additional contribution to the spread of the points in Figure 1.

We use a data set of gradual SEP events observed with the GOES satellite to examine the two factors discussed above which may result in a diminished correlation between peak SEP intensities and CME speeds: enhanced SEP ambient intensities and variations among peak SEP spectra. For the study we use only the SEP events reaching the threshold of 10 protons cm^{-2} sr^{-1} s^{-1} at $E > 10$ MeV used by the National Oceanic and Atmospheric Administration Space Environment Center for environmental forecasting purposes. We preclude the use of enhanced $E < 10$ MeV proton populations observed at 1 AU because they may be produced in corotating interaction regions (CIRs) beyond 1 AU. CIR proton intensities have strong positive heliospheric radial gradients [*Mason and Sanderson*, 1999], with intensities at 1 AU far exceeding those near the Sun, where we want to determine the ambient intensities. We assume here that the ambient SEP intensities measured at 1 AU scale with those present near the Sun, where shock acceleration takes place.

A second reason for using only SEP events at the

NOAA threshold is that we want to compare the $E >$ 10 MeV population with that at higher ($E >$ 60 MeV) energies, which lie below detector thresholds in weaker events. It would be desirable to select a large sample of SEP events accompanied by measured CME speeds, but this was not possible during the period of available GOES data. However, effects of SEP ambient populations and spectral variations can be examined separately from the CME observations, as we do here.

2. Data Selection and Analysis

The SEP events of the study were selected from plots of integral energy channels of the Space Environment Monitor on the GOES 6, 7, and 8 spacecraft from 1986 to 2000, published at the web site http://www.ngdc.noaa.gov/stp/stp.html. We used the NOAA Space Environment Services Center preliminary listing of such events (http://umbra.nascom.nasa.gov-/SEP/seps.html) as a guide to event selection. Since some of those events consist of multiple SEP injections, the SEP event listings of *Cliver and Cane* [1990] and *Gentile et al.* [1993] and event data of *Bazilevskaya et al.* [1990] and *Sladkova et al.* [1998] were also used in the event selections. For both the peak intensities and ambient levels we use the integral $E >$ 10 MeV (I10) and the $E >$ 60 MeV (I60) proton channels of the GOES detectors.

Only the event "prompt" peaks, rather than the peaks often observed later at associated shock passages, were selected for analysis. The goal was to use intensities of SEP events representative of the acceleration of shocks near the Sun, rather than SEP intensities characteristic of shock acceleration regions which have propagated to 1 AU and significantly evolved in the meantime. In some cases the NOAA listed events did not reach the NOAA threshold, and there were cases in which no increase in the $E >$ 60 MeV intensities was obvious. In others, SEP intensities gradually increased until shock passage, with no prompt peak observed prior to the shock. These events were not used in the analysis. On the other hand, all SEP events of several days or more duration were screened for additional SEP injections, and all such injections reaching the NOAA threshold were selected as separate events. Associated solar source region locations and solar event associations were not considered as selection criteria. This resulted in a total of 71 SEP events for the period 1986–2000. Solar source locations, generally based on Hα or X-ray flare locations, were identified for all 71 events. A GOES plot of one of the events, on October 30-31, 1992, is shown in Figure 2.

2.1. Ambient SEPs

Besides the peak prompt I10 and I60 intensities of each event, the ambient intensities observed at those energies, AM10 and AM60, just preceding the onset of the SEP event were also listed. Note that these ambient intensities also consist of instrumental backgrounds

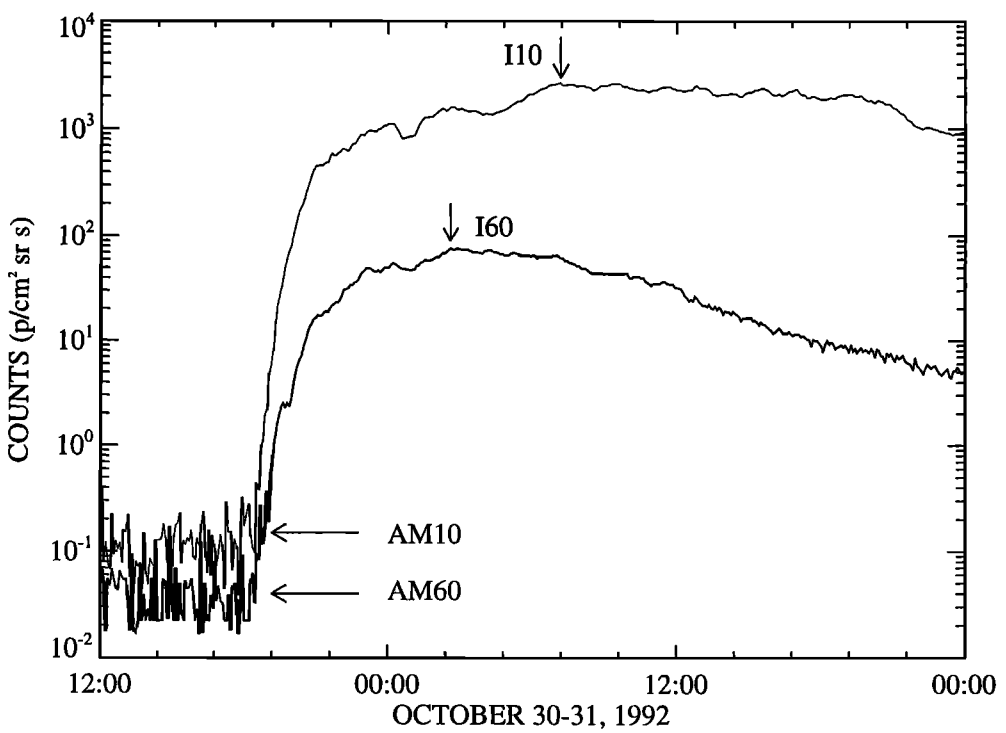

Figure 2. The GOES solar energetic particle (SEP) event of October 30-31, 1992. The vertical arrows mark the times of peak I10 ($E >$ 10 MeV) and I60 ($E >$ 60 MeV) proton intensities. The horizontal arrows show the ambient AM10 and AM60 intensities of the event, which in this case are very near the instrumental backgrounds.

Table 1. Correlation Coefficients and Confidence Levels of Peak Intensities of 71 SEP Events

	I10		I60	
	r	confidence	r	confidence
AM10	0.36	99.8%	0.35	99.7%
AM60	0.28	98.1%	0.40	100.0%

equivalent to ≤ 0.1 and ≤ 0.03 protons cm^{-2} sr^{-1} s^{-1} in the AM10 and AM60 channels, respectively, that we have not attempted to remove. Because of the dynamic ranges involved, only the logs of intensities were used in the correlations. Table 1 gives the correlation coefficients and statistical confidence levels for the four combinations of peak and ambient intensities. Each of the correlations is statistically significant, indicating that the ambient SEP intensities are an important factor in the peak intensities of SEP events.

The two plots with the best correlation coefficients are shown in Figure 3. In each case the dashed lines show the least squares best fits to the data. The diagonal solid lines indicate the points at which the peak intensities equal the ambient intensities; any SEP events below and to the right of those lines are undetectable. Events occurring in the undetectable regions would detract somewhat from the positive correlations of Table 1. We can estimate the number of such unobserved I10 events from the total number of listed NOAA events above intensities of 10 protons cm^{-2} sr^{-1} s^{-1} (149 events) and of 100 protons cm^{-2} sr^{-1} s^{-1} (62 events) and an assumption of average durations for those intensity levels of 2 days and 1 day, respectively. Assuming random occurrence in time throughout the 14.5-year period of the study, the estimated number of unobserved I10 events in Figure 3a is only 1.3 events. The corresponding number of unobserved I60 events will be even smaller, showing that the unobserved SEP events are not a significant factor in the correlations. It is also clear in both plots that the events with small peak intensities decline more rapidly with increasing ambient levels than do the events with large peak intensities. The positive correlations of the peak SEP intensities with the ambient SEP intensities suggest that enhanced ambient SEP intensities are an additional factor contributing to the broad spread in the correlation of SEP peak intensities and CME speeds of Figure 1, especially at the highest peak intensities.

A more definitive test of the possibility that SEP intensities are higher when CME shocks operate in an enhanced ambient SEP population would be to compare the peak intensities to both the associated CME speeds and the associated ambient SEP levels. We would then expect that large peak intensity events with low ambient levels would require generally faster CMEs than would the large peak intensity events with high ambient levels. Unfortunately, we have CME speeds from the SMM [*Burkepile and St. Cyr*, 1993] or the Large-Angle Spectrometric Coronagraph (LASCO) [*Gopalswamy et al.*, 2000] coronagraphs for only a few of the events of the study. For the 17 most intense (I10 > 700 protons cm^{-2} sr^{-1} s^{-1}) events of Figure 3 we have six CME speeds and one lower limit CME speed. All seven of the speeds exceeded 1200 km s^{-1} except for that of March 18, 1989 [*Kahler*, 1993] in which the CME speed was 740 km s^{-1} and the ambient level was enhanced at 200 protons cm^{-2} sr^{-1} s^{-1}. These few CME speeds are at least consistent with a requirement that high-intensity SEP events with low ambient levels must have CMEs of very high speeds, perhaps $v > 1200$ km s^{-1}, while those with high ambient levels may be associated with CMEs of lower speeds.

2.2. Energy Spectral Variations

We can determine whether variations of the energy spectra of the SEP events contribute to the scatter of points in Figure 1. Figure 4 is a plot of the log I60 peak proton intensities versus the log I10 peak proton intensities for all 71 events. The least squares best fit is close to that for a differential energy power law spectral exponent of $\gamma = 3$. The scatter of points is about one unit in the log both above and below the best fit line, suggesting that if we had a high correlation between log I10 and log v, where v is the CME speed, then we would get a scatter of up to two units of log I60 in the correlation of log I60 and log v. We have no reason to take any energy threshold as preferential in the correlation of SEP intensities with v, but we conclude that the spectral variation among SEP events should account for at least one unit in the variation of the logs of the peak intensities.

We can proceed further to look for systematic behavior in these spectral variations. If we treat the two variables of Figure 4 as equally independent [*Bevington*, 1969], then the least squares best fit slope of Figure 4 is $s = 1.23 = d\log(\text{I60})/d\log(\text{I10})$, indicating flatter energy spectra with increasing event peak intensities. Assuming that the integral number size distribution of I10 events is $N = A(\text{I10})^{-\alpha}$, then $d\log N = -\alpha d\log(\text{I10}) = -\alpha s^{-1} d\log(\text{I60})$, where A and α are constants. This means that we expect the integral number size distribution of I60 SEP events to be flatter than that of the I10 events by about the factor $s = 1.23$. Figure 5 shows the distributions for I10 and I60 for the events of this study. The best fit slope for the 62 I60 events exceeding peak intensities of 0.3 protons cm^{-2} sr^{-1} s^{-1} is -0.266 ± 0.017. The I10 events are shown plotted in a manner similar to the plot of 225 SEP events by *Smart and Shea* [1997] in which they reported a break in their distribution at I10 = 1000 protons cm^{-2} sr^{-1} s^{-1} and a slope of -0.47 for the lower-intensity events. We also find a break in the size distribution of the 71 I10 events, but

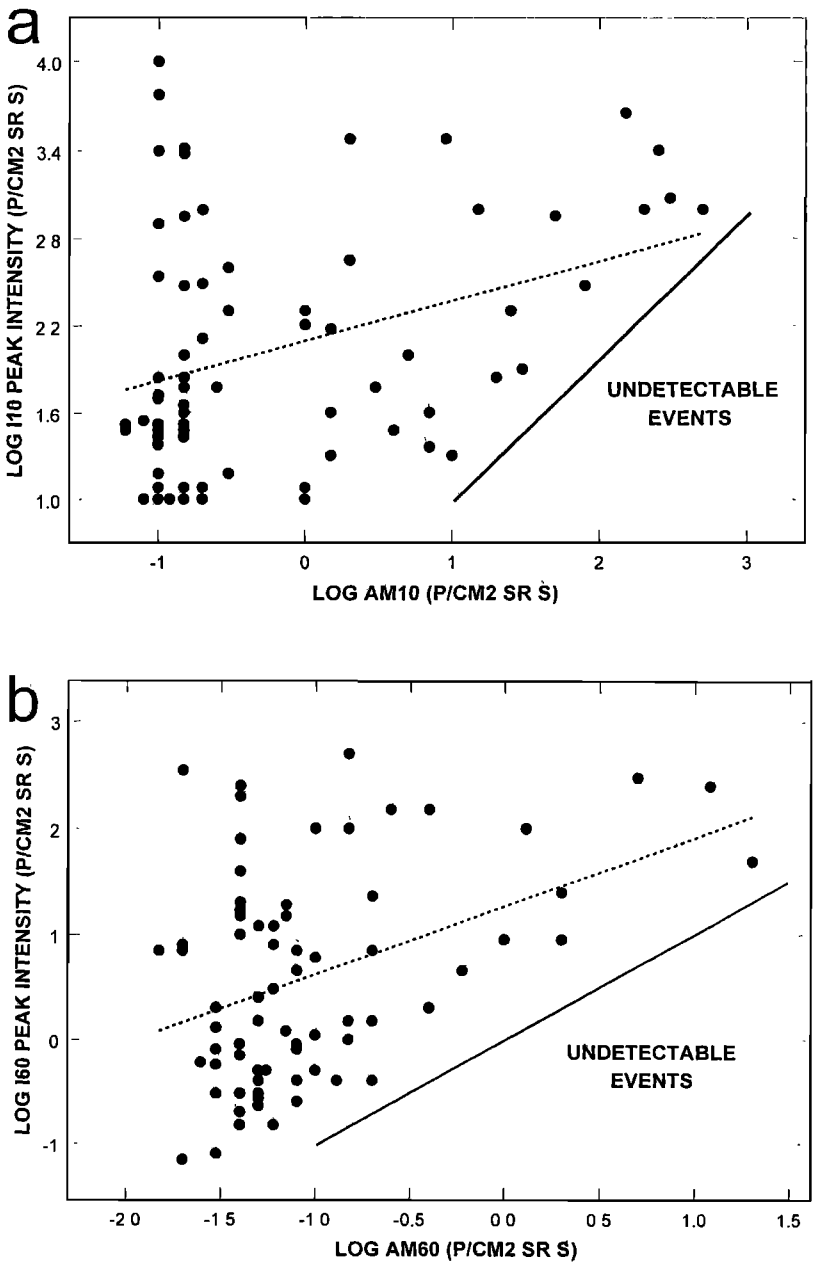

Figure 3. (a) Correlation of peak $E > 10$ MeV SEP intensities (I10) with the $E > 10$ MeV ambient SEP intensities (AM10). The dashed line is the least squares best fit of log(I10) = 0.27 log(AM10) + 2.10, and the solid line shows where the peak intensity equals the ambient intensity. (b) The same as Figure 3a but for the peak $E > 60$ MeV SEP intensities (I60) and $E > 60$ MeV ambient SEP intensities (AM60). The dashed line is the least squares best fit of log(I60) = 0.65 log(AM60) + 1.27.

at I10 $\sim$ 2000 protons cm^{-2} sr^{-1} s^{-1}, and the best fit slope for the lower intensities is -0.360 ± 0.012; for all points it is -0.573 ± 0.069. These steeper fits to the I10 number distributions confirm the trend toward flatter energy spectra with increasing SEP peak intensities suggested by the plot of Figure 4.

Variations of SEP energy spectral indices γ with solar source longitude were obtained by *Van Hollebeke et al.* [1975] and by *Cane et al.* [1988], showing generally that eastern hemisphere SEP events have larger γ, i.e., steeper energy spectra than western hemisphere events. That result indicates that variations in energy spectra coupled to solar source longitudes also play a role in the scatter of Figure 1. In Figure 6 the plot of γ against solar longitude for the events of this study shows a slow decrease toward western longitudes. The least squares best fit shown on the plot is $\gamma = -0.004L + 3.04$, where L is the solar longitude, and the correlation coefficient

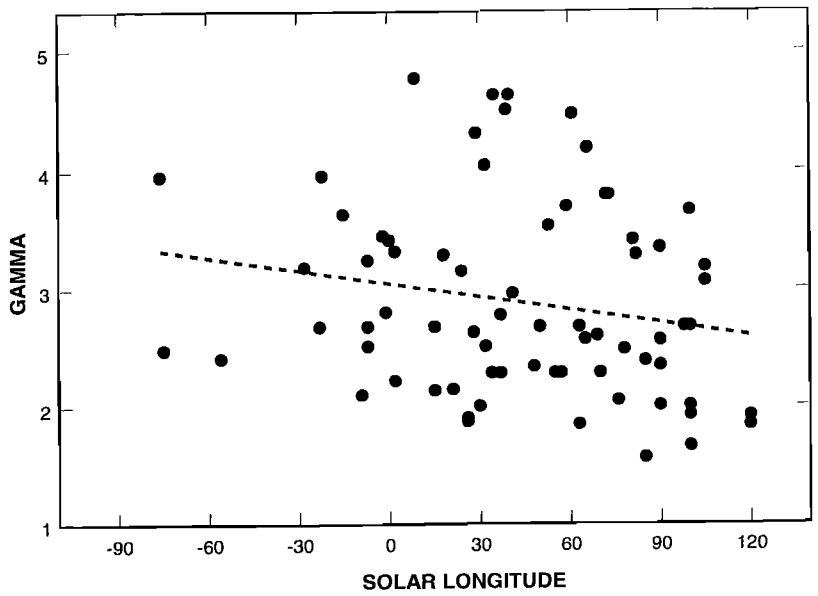

Figure 4. Plot of peak $E > 60$ MeV SEP intensities versus the corresponding $E > 10$ MeV SEP intensities of the 71 events of the study. The least squares best fit (dashed line) of log (I60) = 0.96 log(I10) − 1.38 is close to that of log(I60) = log(I10) − 1.56 for differential power law spectra with $\gamma = 3$.

is $r = 0.21$. The range of values of γ at all longitudes clearly exceeds the small decline of average values with increasing solar longitude.

3. Discussion

A relationship between peak SEP intensities and associated CME speeds has been found, despite the inherent limitations of such a comparison given in section 1. As Figure 1 shows, different data sets yield similar results, with the log of the SEP intensity scaling to the log CME speed with a slope of $\sim$ 4–5. Since these simple relationships must result from some basic physics of shock acceleration, it is important to determine other factors important for the resulting peak SEP intensities. The uncertainties in determining true CME and shock speeds by measuring the CME speeds in the plane of the sky have been noted by others. Here we identify two other factors, enhanced SEP ambient intensities and SEP energy spectral variations, that appear to contribute to the spread of points in Figure 1.

As discussed in section 1, an enhanced ambient source population of energetic particles has been suggested by others as an explanation of some observational results at and beyond 1 AU. We interpret the correlation in Figure 3 as the result of shock acceleration acting on an enhanced source population of SEPs. This interpretation may also be applicable to three complex SEP events discussed by *Kahler* [1993], in each of which large (I10 > 1000 protons cm^{-2} sr^{-1} s^{-1}) $15 < E < 44$ MeV SEP events with well connected (20°W to 70°W) solar source regions had unusually long rise times. In each case a relatively fast ($v > 700$ km s^{-1}) CME was associated with the onset of a SEP event with a long rise phase. During each rise phase a second, slower ($v < 700$ km s^{-1}) CME was observed in association with an apparent inflection of the rise phase profile of the SEP event. *Kahler* [1993] suggested only that the long rise time resulted from SEP acceleration by the second CME-driven shock, but it is possible that the very high peak intensity of I10 was achieved because the first CME shock produced an enhanced SEP population that served as the seed population for the second CME of relatively modest speed.

An alternative interpretation of the role of ambient SEPs is that sequences of very fast ($v > 1200$ km s^{-1}) CMEs occur closely together in time, so that several large SEP events would be independently initiated during the decay phases of earlier large SEP events. This may have happened in October 1989 when a large (I10 = 2500 protons cm^{-2} sr^{-1} s^{-1}) SEP event on October 19 was followed by subsequent SEP events on October 22, 24, and 29. CME speeds were measured only for the October 24 event, but that CME speed was 1956 km s^{-1} [*Burkepile and St. Cyr*, 1993], suggesting a CME sufficiently fast to produce an intense SEP event, regardless of the SEP ambient level. The several events shown in the upper left part of Figure 3a with high I10 and low AM10 make clear that an observed enhanced ambient SEP population is not a requirement for a CME shock to produce a large (I10 > 1000 protons cm^{-2} sr^{-1} s^{-1}) SEP event.

The role of the ambient SEPs can be assessed only when both CME speeds and ambient SEP levels are available for a significant sample of large SEP events. As discussed in section 2.1, the lack of an inverse correlation between CME speed and SEP ambient levels

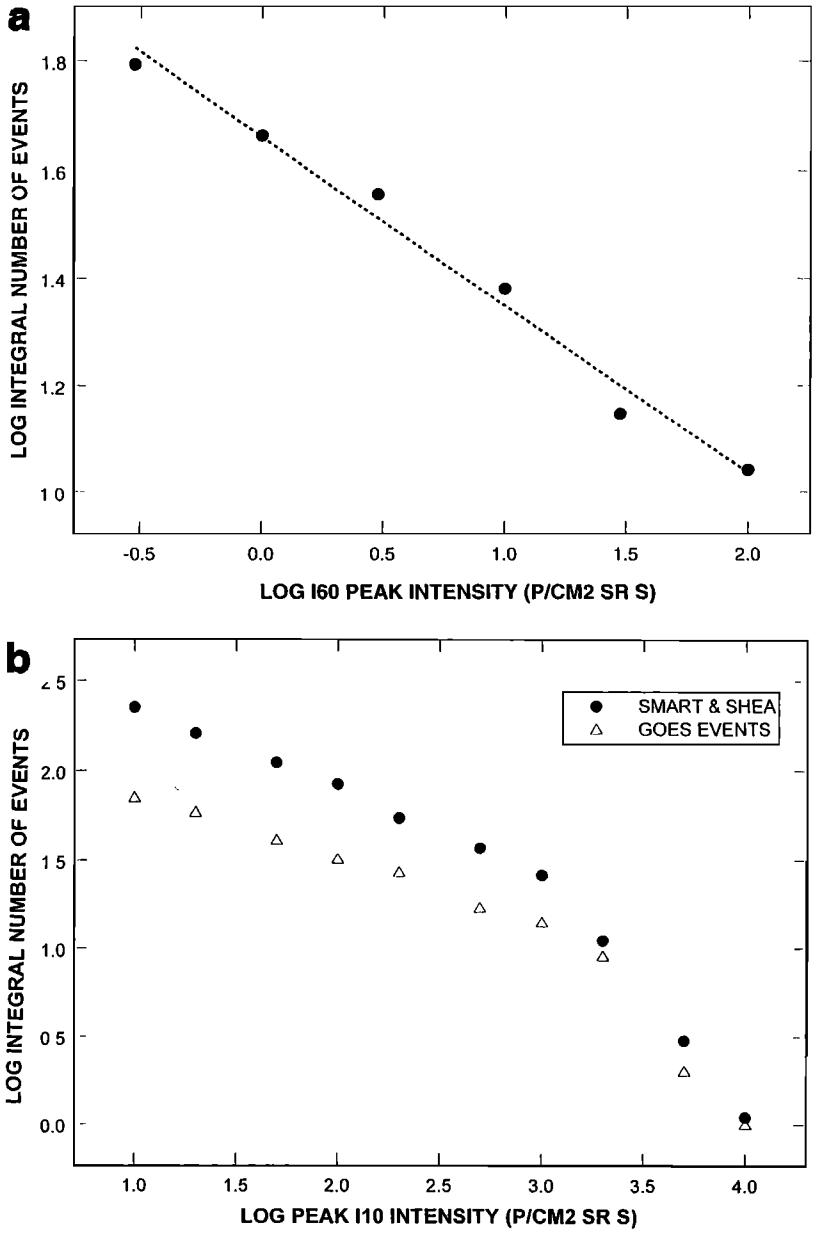

Figure 5. (top) The integral number distribution for 62 I60 events with the least squares best fit shown by the dashed line. (bottom) The integral number distribution for 225 I10 events over three solar cycles from *Smart and Shea* [1997] and the 71 I10 events of this study. The least squares best fit slope of the spectrum below 1000 protons cm^{-2} sr^{-1} s^{-1} is − 0.47 for the 225 events. The least squares best fit to the spectrum below 2000 protons cm^{-2} sr^{-1} s^{-1} is − 0.36 for the 71 events.

for the large SEP events would make it unlikely that SEP ambient populations play a causal role in the SEP peak intensities. If there are sufficient differences of elemental abundances or charge states observed among gradual SEP events, then a comparison of SEP event characteristics with their corresponding preevent characteristics might also be useful in determining the role of enhanced ambient SEPs.

We also identify variations in SEP energy spectra shown in Figure 4 as a second factor contributing to the broad range of values of log I versus log v of Figure 1. The correlation coefficient of the log I versus log v plot is higher for the 20-MeV protons than for the 2-MeV protons shown in Figure 1, but the dependence of the correlation coefficient on SEP energy has not been systematically examined. In this work we have used only GOES energy ranges of $E > 10$ MeV and $E > 60$ MeV, but the range of the data points of Figure 4 suggests that spectral variations of SEP events account for at least one of the ~ 4 orders of magnitude of the spread of values of log I in Figure 1.

The statistical trend toward flatter SEP energy spec-

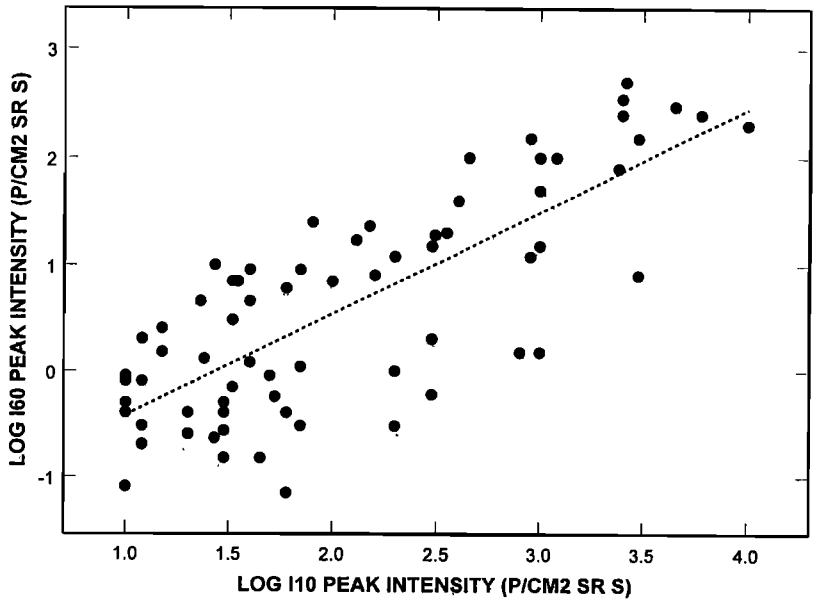

Figure 6. Distribution with solar longitude of the spectral index γ for an assumed differential power law fit of $dN/dE = AE^{-\gamma}$ using peak values of I10 and I60. The dashed line is the least squares best fit to the 71 SEP events of the plot.

tra with increasing peak intensities is consistent with the streaming-limited intensities at low ($E < 10$ MeV) energies observed by *Reames and Ng* [1998]. Their observed dearth of 4–9 MeV SEP intensities exceeding 400 protons cm^{-2} sr^{-1} s^{-1} MeV^{-1} implies that the largest SEP events will have flatter spectra resulting from the streaming limitations at low energies. If we assume power law differential energy spectra with exponents of γ of 2–3, then the observed streaming limit implies a cutoff in $E > 10$ MeV events at $\sim$ 1000 protons cm^{-2} sr^{-1} s^{-1}, where we and *Smart and Shea* [1997] find a break in the size distribution of the I10 events (Figure 5, bottom). No size-distribution cutoff is found at the higher I60 energy range (Figure 5, top), also consistent with a streaming limitation confined to lower energies.

We expect a systematic variation of values of γ with solar source longitude, as found by *Van Hollebeke et al.* [1975]. The results of Figure 6 are qualitatively similar to those of *Van Hollebeke et al.* [1975] and of *Cane et al.* [1988], but those authors used spectra at the shock peaks when the peak intensities occurred at shock passages, while we have used only event peaks preceding shocks. Contrary to the result of *Van Hollebeke et al.* [1975], we do not see a minimum in γ associated with well-connected events near 50°W but a small decrease toward the western hemisphere with a large spread in values. This progressive decrease of spectral index from eastern to western longitudes is also consistent with the three longitudinal plots of numbers of SEP events with $E > 1$ GeV, 100 MeV, and 10 MeV by *Smart and Shea* [1996]. While they emphasized the peak in the number distribution of the $E > 1$ GeV events at 60°W, their data are also consistent with the gradual decline of γ across that region toward the west limb.

This longitudinal effect, although weak, is probably due to the change from quasi-perpendicular shocks for the easternmost events to quasi-parallel shocks for the westernmost events [*Reames,* 1999], the peak intensities of which are observed hours to tens of hours after onset times, when shocks are more than 0.1 AU from the Sun. The important question with regard to Figure 1 is how I10 or I60 peak intensities vary with longitude. We find that the average log peak I60 intensity increases by 0.45 (a factor of 2.8 in linear counting rates) from central meridian to 100°W, while the log peak I10 intensity increases by 0.16 (a factor of 1.4 in linear counting rates) over the same range. This is somewhat fortuitous for the correlation of Figure 1 since the increase of average SEP intensities with approach of the source region to the west limb is offset by the corresponding increase of average measured CME speeds [*Gopalswamy et al.,* 2000]. It explains why the two data sets of Figure 1 overlap so closely, even though the Helios/Solwind events were confined to near the solar limbs [*Reames et al.,* 1997] while the Wind/LASCO events included many disk events as well as limb events [*Gopalswamy et al.,* 2000].

4. Summary

The peak intensity of an SEP event observed at 1 AU depends on several factors, one of which is the speed of the CME driving the interplanetary shock. An enhanced ambient SEP population, serving as seed particles for a fast CME shock, is a candidate factor for

subsequent high-intensity SEP events. Accompanying CME speeds, not available for most SEP events of this study, are needed to test this possibility. Variations of energy spectra among the SEP events account for at least 1 of the 4 orders of magnitude of variations in the correlation of log I and log v of Figure 1. The spectral hardening with increasing peak intensity is consistent with streaming-limited intensities at low energies. However, the small statistical increases in peak intensities and spectral hardness toward western solar longitudes are not significant factors for the correlation of Figure 1.

Acknowledgements. Janet Luhmann thanks Volker Bothmer and another referee for their assistance in evaluating this paper.

References

Bazilevskaya, G.A., et al., Solar Proton Events Catalogue 1980–1986, 204 pp., Sov. Geophys. Comm., Acad. Sci. USSR, World Data Cent. B, Moscow, 1990.

Bevington, P.R., *Data Reduction and Error Analysis for the Physical Sciences,* 336 pp., McGraw-Hill, New York, 1969.

Burkepile, J.T., and O.C. St. Cyr, A revised and expanded catalogue of mass ejections observed by the Solar Maximum Mission coronagraph, *NCAR/TN-369+STR,* 233 pp., Nat. Cent. for Atmos. Res., Boulder, Colo., 1993.

Cane, H.V., D.V. Reames, and T.T. von Rosenvinge, The role of interplanetary shocks in the longitude distribution of solar energetic particles, *J. Geophys. Res., 93,* 9555, 1988.

Cliver, E.W., and H.V. Cane, X-class soft X-ray bursts and major proton events during solar cycle 21, in *Solar-Terrestrial Predictions: Proceedings of a Workshop at Leura, Australia,* vol. 1, edited by R.J. Thompson et al., pp. 359-370, Natl. Oceanic and Atmos. Admin., Boulder, Colo., 1990.

Desai, M.I., et al., Particle acceleration at corotating interaction regions in the three-dimensional heliosphere, *J. Geophys. Res., 103,* 2003, 1998.

Gentile, L.C., J.M. Campbell, E.W. Cliver, and H.V. Cane, X-class soft X-ray bursts and major proton events during solar cycle 22 (1987-1991), in *Solar-Terrestrial Predictions - IV,* vol. 2, edited by J. Hruska et al., pp. 153-161, Natl. Oceanic and Atmos. Admin., Boulder, Colo., 1993.

Giacalone, J., and J.R. Jokipii, Spatial variation of accelerated pickup ions at co-rotating interaction regions, *Geophys. Res. Lett., 24,* 1723, 1997.

Gopalswamy, N., M.L. Kaiser, B.J. Thompson, L.F. Burlaga, A. Szabo, A. Lara, A. Vourlidas, S. Yashiro, and J.-L. Bougeret, Radio-rich eruptive events, *Geophys. Res. Lett., 27,* 1427, 2000.

Kahler, S.W., Coronal mass ejections and long risetimes of solar energetic particle events, *J. Geophys. Res., 98,* 5607, 1993.

Kahler, S.W., Coronal mass ejections and solar energetic particle events, in *High Energy Solar Physics,* edited by R. Ramaty, N. Mandzhavidze, and X.-M. Hua, *AIP Conf. Proc., 374,* 61-77, 1996.

Kahler, S.W., J.T. Burkepile, and D.V. Reames, Coronal/interplanetary factors contributing to the intensities of $E > 20$ MeV gradual solar energetic particle events, *Proc. Int. Conf. Cosmic Rays 26th, 6,* 248, 1999.

Kahler, S.W., D.V. Reames, and J.T. Burkepile, A role for ambient energetic particle intensities in shock acceleration of solar energetic particles, in *High Energy Solar Physics: Anticipating HESSI,* edited by R. Ramaty and N. Mandzhavidze, *Astron. Soc. Pac. Conf. Ser., 206,* 468-474, 2000.

Lario, D., R.G. Marsden, T.R. Sanderson, M. Maksimovic, B. Sanahuja, A. Balogh, R.T. Forsyth, R.P. Lin, and J.T. Gosling, Energetic proton observations at 1 and 5 AU, 1, January–September 1997, *J. Geophys. Res., 105,* 18,235, 2000.

Lee, M.A., Particle acceleration and transport at CME-driven shocks, in *Coronal Mass Ejections, Geophys. Monogr. Ser.,* vol. 99, edited by N. Crooker, J.A. Joselyn, and J. Feynman, pp. 227-234, AGU, Washington, D.C., 1997.

Mason, G.M., and T.R. Sanderson, CIR associated energetic particles in the inner and middle heliosphere, *Space Sci. Rev., 89,* 77, 1999.

Mason, G.M., J.E. Mazur, and J.R. Dwyer, ^{3}He enhancements in large solar energetic particle events, *Astrophys. J., 525,* L133, 1999.

Reames, D.V., Particle acceleration at the Sun and in the heliosphere, *Space Sci. Rev., 90,* 413, 1999.

Reames, D.V., Particle acceleration by CME-driven shock waves, in *Invited, Rapporteur, and Highlight Papers,* edited by B.L. Dingus, D.B. Kieda, and M.H. Salamon, *AIP Conf. Proc., 516,* 289-300, 2000.

Reames, D.V., and C.K. Ng, Streaming-limited intensities of solar energetic particles, *Astrophys. J., 504,* 1002, 1998.

Reames, D.V., S.W. Kahler, and C.K. Ng, Spatial and temporal invariance in the spectra of energetic particles in gradual solar events, *Astrophys. J., 491,* 414, 1997.

Sladkova, A.I., et al. (Eds.), *Catalogue of Solar Proton Events 1987-1996,* 246 pp., Moscow Univ. Press, Moscow, 1998.

Smart, D.F., and M.A. Shea, The heliolongitudinal distribution of solar flares associated with solar proton events, *Adv. Space Res., 17*(2), 113, 1996.

Smart, D.F., and M.A. Shea, The > 10 MeV solar proton event peak flux distribution, in *Solar-Terrestrial Predictions - V,* edited by G. Heckman et al., pp. 449-452, Reg. Warning Cent. Tokyo, Ibaraki, Japan, 1997.

Van Hollebeke, M.A.I., L.S. Ma Sung, and F.B. McDonald, The variation of solar proton energy spectra and size distribution with heliolongitude, *Sol. Phys., 41,* 189, 1975.

S. W. Kahler, AFRL/VSBS, 29 Randolph Road, Hanscom AFB, MA 01731. (Stephen.Kahler@hanscom.af.mil)

(Received July 17, 2000; revised August 31, 2000; accepted September 13, 2000.)